Topological surface states revealed by Sb thin films adsorbed with impurity atoms

Chi-Hsuan Lee and Chih-Kai Yang*
Graduate Institute of Applied Physics, National Chengchi University, Taipei 11605, Taiwan, Republic of China
(Received 15 October 2012; published 12 March 2013)

The prevalent concept is that a topological insulator is made of thick layers of atoms so that its surfaces, where electrical conduction occurs, can be distinguished from the insulating bulk of the interior. One important reason is that the thin film topological insulator may cause the opening of energy band gaps by quantum tunneling between the two surfaces. Inspired by an experiment on antimony thin films, we use density functional calculations to investigate the electronic structure of the four-bilayer Sb film and find that adsorptions of nonmagnetic impurity atoms of hydrogen and 3*d* transition-metal atoms on the film all close the energy gap of the free-standing film and facilitate the formation of Dirac cones that preserve time-reversal symmetry. However, magnetic atoms of the 3*d* transition metals do just the opposite. The results suggest the counterintuitive concept of achieving topological conduction by doping nonmagnetic impurity atoms on thin films of topological insulators.

DOI: 10.1103/PhysRevB.87.115306 PACS number(s): 73.20.At, 73.20.Hb

Surface states of a topological insulator[1–9] are typically represented by Dirac cones in the energy gap of the bulk electronic band structure. The electron states of the linear crossing bands possess time-reversal symmetry and hence guarantee nondissipative transport against the presence of impurity atoms and geometric perturbations. Potential applications of the topological surface states include spin-polarized transport, quantum computing, and the more subtle manifestation of Majorana fermions.[10] However, the topological insulator has to have large enough dimensions so that the conducting surface states can be unambiguously separated from the bulk states and have all the characters of topological conduction. This requirement in size sometimes means tens of nanometers in thickness that a very thin film does not have.

Thin films, nonetheless, have the advantage of being easier to synthesize and convenient for making miniaturized devices, but the reduced thickness also means increased coupling between the two surfaces, which may reach the point of destroying the Dirac cones and opening a band gap in the surface states. Furthermore, a pristine film synthesized without the contamination of impurity atoms is sometimes difficult to achieve. Even if that is possible, the sample still has to face the possibility of exposure to foreign atoms in some applications.[11] Knowing better how the thickness and adatoms affect the surface electronic structure of the thin film is thus important for studies in and potential applications of topological conduction.

In this regard, experiments performed by Bian *et al*. have shown that pristine Sb films as thin as four bilayers can be successfully synthesized over a Bi-terminated Si (111) surface.[12] Their angle-resolved photoemission spectroscopy indicates that a Dirac cone is formed close to the Fermi level. However, their calculation based on density functional theory (DFT) also shows that a free-standing Sb film consisting of four bilayers opens a band gap in the surface states due to tunneling-induced coupling between the top and bottom surfaces. Theoretically, one can try to close the gap by increasing the thickness of the film. However, if the thickness of four bilayers is to be maintained, the gap will also disappear by applying hydrogen termination of the Sb film. The latter result clearly points to the crucial role played by the substrate and, in a more general sense, adsorbed atoms in forming and shaping topological surface states of thin films that would otherwise be topologically trivial and therefore warrants a wider investigation in this direction.

In our study on the consequences of the adsorption of foreign atoms, we first wanted to know how different configurations of H adsorption affect the surface states of the four-bilayer Sb film. We used spin-polarized DFT calculations as implemented in the Vienna *Ab initio* Simulation Package codes[13,14] as our tools. The important spin-orbit interaction was included in the calculation and local-density approximation selected for the exchange-correlation potential. To accommodate various configurations involving H adsorption, an expanded unit cell of 32 Sb atoms was used. Cutoff energy was set at 300 eV and a $9 \times 9 \times 1$ sampling of **k** points in the first Brillouin zone was also adopted. Relaxation of the atomic positions in the Sb films with and without impurity atoms was always executed before relevant energy bands were calculated.

The left part of Fig. 1(a) shows the energy bands of the pristine four-bilayer Sb film along the $\bar{\Gamma} - \bar{M}$ direction, with projected Sb bulk states superimposed in shaded regions. Around the $\bar{\Gamma}$ point, two bands are found between the shaded areas and thus represent surface states of the Sb film. However, an energy gap of 47.5 meV due to quantum tunneling between the two faces of the film separates the two doubly degenerate bands. If we increased the thickness of the film to five and six bilayers [as represented by the corresponding band structures in the middle and right parts of Fig. 1(a)] and thus reduced the tunneling, the gap shrank to 31.1 and 15.8 meV, respectively, in accordance with the reported trend in Ref. 12. As with the four-bilayer film, each of the two surface bands was doubly degenerate and occupied by electrons with both spin directions.

With the adsorption of H atoms, the conduction of the Sb film was drastically different. Three configurations of H adsorption were considered in our calculation. In the first case, a single H atom was attached to a Sb atom in the bottom surface layer of the film in the expanded unit cell of 32 Sb atoms. Shown in Fig. 1(b), the bond length between the Sb and H is found to be 1.736 Å, and the binding energy is 1.687 eV per H atom per unit cell. Such a firm adsorption indicated strong interaction between the adatom and the host. Most importantly, a Dirac cone was clearly formed as a result, as shown in

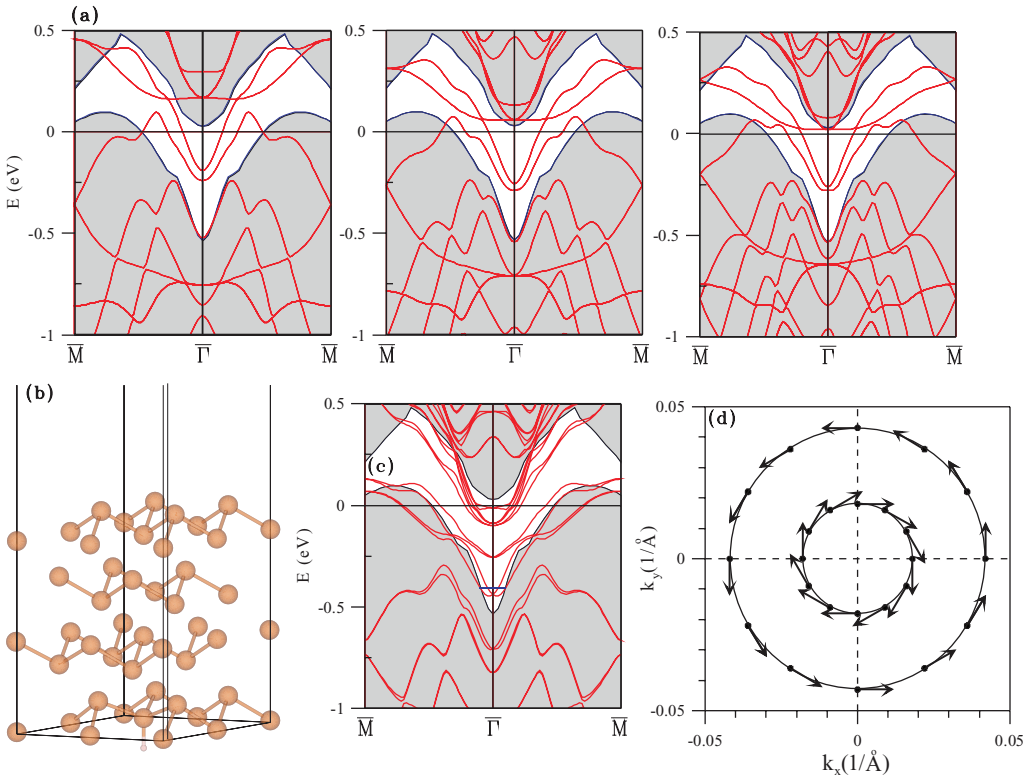

FIG. 1. (Color online) (a) Energy bands of the four-, five-, and six-bilayer Sb films (from left to right) along the $\bar{\Gamma} - \bar{M}$ direction, with projected bulk Sb states superimposed in the shaded area. The band gap shrinks as the thickness of the film increases. (b) An H atom is adsorbed on the bottom face of the four-bilayer Sb film in a unit cell of 32 Sb atoms. (c) Energy bands of the configuration shown in (b) have the gap closed and a Dirac cone formed. (d) Spin texture of the configuration is revealed in the k_x-k_y plane by two concentric equi-energy circles corresponding to the energy specified by the horizontal bar in (c).

Fig. 1(c), where two bands mostly within the gap between the shaded areas cross each other at 0.440 eV below the Fermi level. Analysis of the composition of the wave functions revealed that the two bands were almost entirely composed of electrons from the top surface without the H adatoms. In fact, only in **k** points approaching the Brillouin zone boundary did electrons from the bottom Sb surface with H adatoms make an appreciable contribution to the two bands. This strong suppression of quantum tunneling[12] between the two surfaces of the film destroyed symmetry along the normal to the film and lifted degeneracy of the bands of the pristine film, forming Dirac cones as a results. Moreover, the conduction over the uncontaminated surface layer was then protected by time-reversal symmetry. An analysis of the spin texture[15] of the topological surface states was performed by extracting **k** points of energy equal to -0.406 eV. In Fig. 1(d) the **k** points corresponding to the energy form two concentric equi-energy circles centered at $\bar{\Gamma}$ in the k_x-k_y plane with the spin at each point locked perpendicularly to the direction of the crystal momentum. The fact that each spin angular momentum had no component along the k_z axis and the spin direction at point **k** was totally opposite to that of $-\mathbf{k}$ assured the complete disappearance of 180° elastic backscattering of the surface electrons and facilitated nondissipative conduction.

If there were more than one H atom adsorbed on the surface per unit cell, the binding energy for each adsorbed H atom increased to 1.907 eV for 2 H and dropped to 1.872 eV for four H per unit cell in our calculation, and the optimal configurations after the relaxation process had the Sb-H bonds deviated from the normal to the surface. Shown in Figs. 2 and 3 are the configurations for two H and four H adsorptions in the expanded unit cell as well as the energy bands and spin texture, with each having a Dirac cone between the shaded regions. The figures also show that time-reversal symmetry is still preserved for the surface states, but the projections of constant energy surfaces over the k_x-k_y plane are no longer circles but more like distorted ellipses, reflecting the asymmetry introduced by the additional H adatoms. The spin is no longer necessarily orthogonal to **k** and appreciable out-of-plane components also appear from the calculation.

Naturally, a question arose about whether adsorption of atoms other than H would also produce Dirac cones and nondissipative conduction on the Sb film. To address the issue, we further included all 3*d* transition metals (TM) as individual adsorbates in our investigation. In each case, a single TM atom was adsorbed on the top surface of the four-bilayer Sb film in the same expanded unit cell. Each configuration was relaxed, and the corresponding energy bands and spin texture analyzed.

Table I provides information about the binding energy, charge transfer, and magnetic moment for each of the 3*d* TM adsorbates from the calculation. As in the case of H adsorption, binding energy was derived by subtracting the total energy of the doped Sb film from the sum of total energies of the pristine Sb film and the free TM atom. It is obvious from the listed

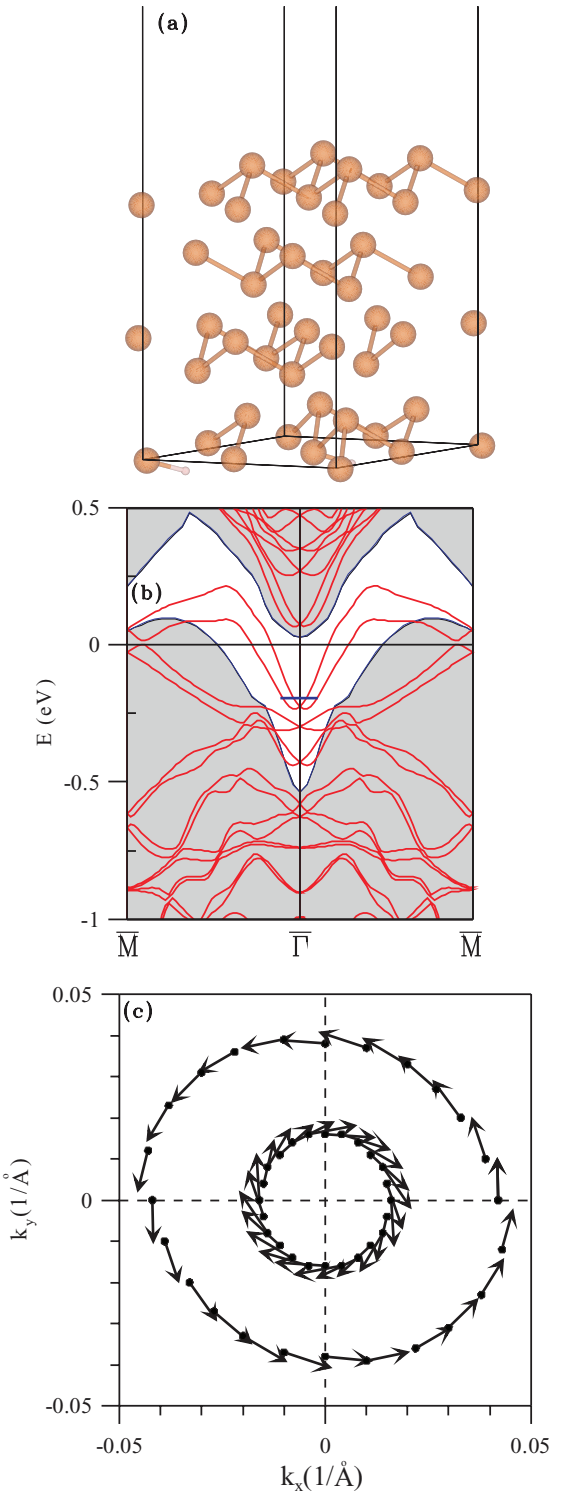

FIG. 2. (Color online) (a) Two H atoms are adsorbed on the bottom face of the four-bilayer Sb film in a unit cell of 32 Sb atoms. (b) Energy bands of the configuration shown in (a). (c) Spin texture corresponding to the energy specified by the horizontal bar in (b).

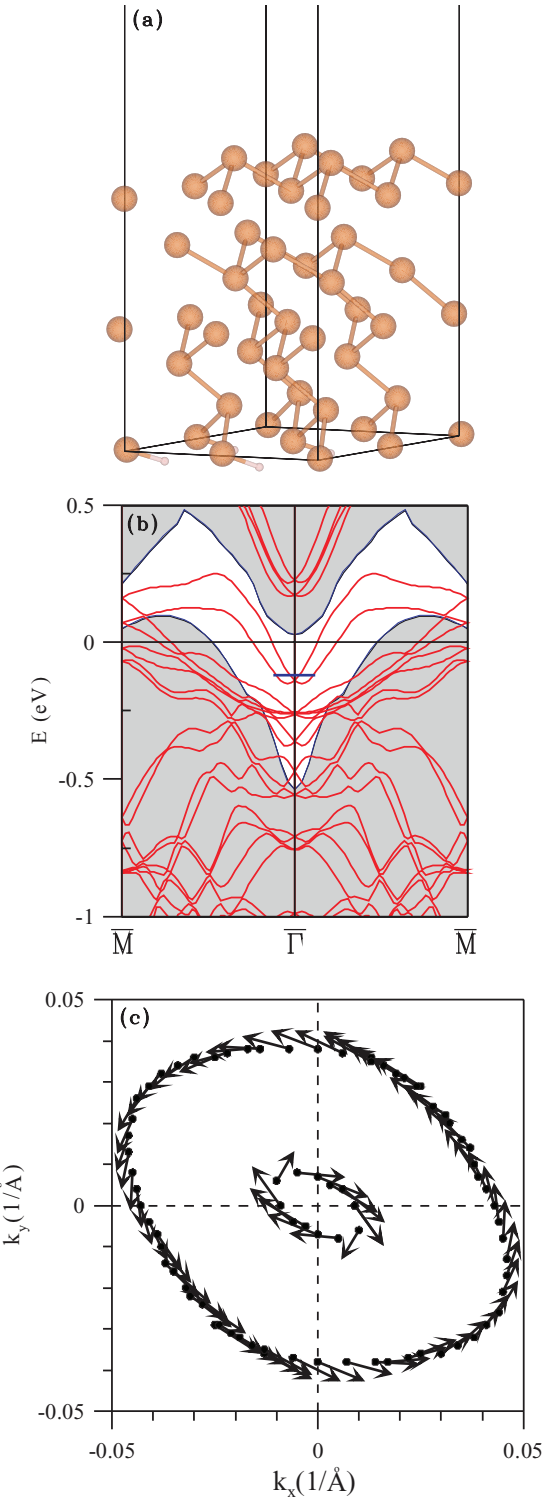

FIG. 3. (Color online) (a) Four H atoms are adsorbed on the bottom face of the four-bilayer Sb film in a unit cell of 32 Sb atoms. (b) Energy bands of the configuration shown in (a). (c) Spin texture corresponding to the energy specified by the horizontal bar in (b).

high binding energies that almost all TM-doped Sb films are robust structures, with the only exception of Zn. Bader charge analysis[16] also points to a trend, with the only exception of Cr, that higher binding energy is generally associated with larger charge transfer between the TM and Sb film, regardless of the sign of charge. Thus, the Sc-adsorbed film has the highest binding energy of 7.890 eV due to the transfer of more than one electron (1.0781 e) from the Sb film to the Sc atom, while Zn

TABLE I. Binding energies E_b, charge transfers ΔQ, and magnetic moments M_{tot} of the four-bilayer Sb film adsorbed with $3d$ TM atoms.

	Sc	Ti	V	Cr	Mn
E_b (eV/atom)	7.890	4.981	3.910	2.747	3.090
ΔQ (e)	1.0780	−0.8140	−0.5005	−0.3101	−0.1140
M_{tot} (μ_B)	0.0003	0.6004	1.2350	4.0493	3.1366
	Fe	Co	Ni	Cu	Zn
E_b (eV/atom)	4.430	6.062	5.113	3.145	0.807
ΔQ (e)	0.2032	0.3211	0.2917	0.0991	−0.0488
M_{tot} (μ_B)	2.0496	0.0021	0.0000	0.0000	0.0000

is least bonded to the film as a result of the smallest transfer of charge. Also listed in Table I are magnetic moments per unit cell for the TM-adsorbed Sb films. No magnetism is associated with the adsorption of a Ni, Cu, or Zn atom, and Sc or Co adsorption contributes only a very small magnetic moment. The other TM atoms, however, magnetize the unit cell substantially, leading to serious violation of time-reversal symmetry.

We first examined the electronic structures of Sb films with nonmagnetic adsorption. A typical example was provided by a single Cu atom, shown in Fig. 4(a), adsorbed on the top surface of the four-bilayer Sb film in the same expanded unit cell. Relaxation of the whole structure places the Cu atom in a position having three Sb atoms as nearest neighbors. Binding energy was calculated to be 3.145 eV per Cu atom and thus indicated a robust binding. Two Dirac cones [Fig. 4(b)], both centered at the $\bar{\Gamma}$ point and below the Fermi level, were spotted as a result of the Cu adsorption. The one lower in energy was found overwhelmingly to comprise wave functions from electrons in the surface layer without the Cu adatom, and only in **k** points close to the Brillouin zone boundary and of energy above the Fermi level did electrons from the surface with the Cu adatom make an appreciable contribution to the energy bands associated with the cone, proving, once again, suppression of quantum tunneling occurred. The Dirac cone with higher energy had more wave functions from Cu and thus represented more of the surface with Cu adsorption.

It is, thus, feasible, by adjusting the Fermi level, to promote nondissipative conduction along, for example, the $\bar{\Gamma} - \bar{M}$ direction in the surface layer without the adsorbed Cu. The relevant energy bands are spin polarized and invariant under time reversal. Analysis of spin texture at constant energy confirms the time-reversal symmetry by two projected concentric equi-energy circles centered at the $\bar{\Gamma}$ point on the k_x-k_y plane and spin-locked chiral structure. A typical example is shown in Fig. 4(c), where the two concentric circles correspond to the energy of 0.360 eV below the Fermi level. Each spin is orthogonal to its associated **k** vector and has no out-of-plane component. For the Dirac cone of higher energy, the spin texture is warped by appreciable spin components out of the plane, but time-reversal symmetry still remains, giving a picture of topological conduction on both surfaces of the film. Figure 4(d) gives a panorama of energy bands along some symmetry directions of the Brillouin zone. It shows that the contributions to energy bands from the adsorbed Cu atoms, as indicated by the size of circles, are mostly low in

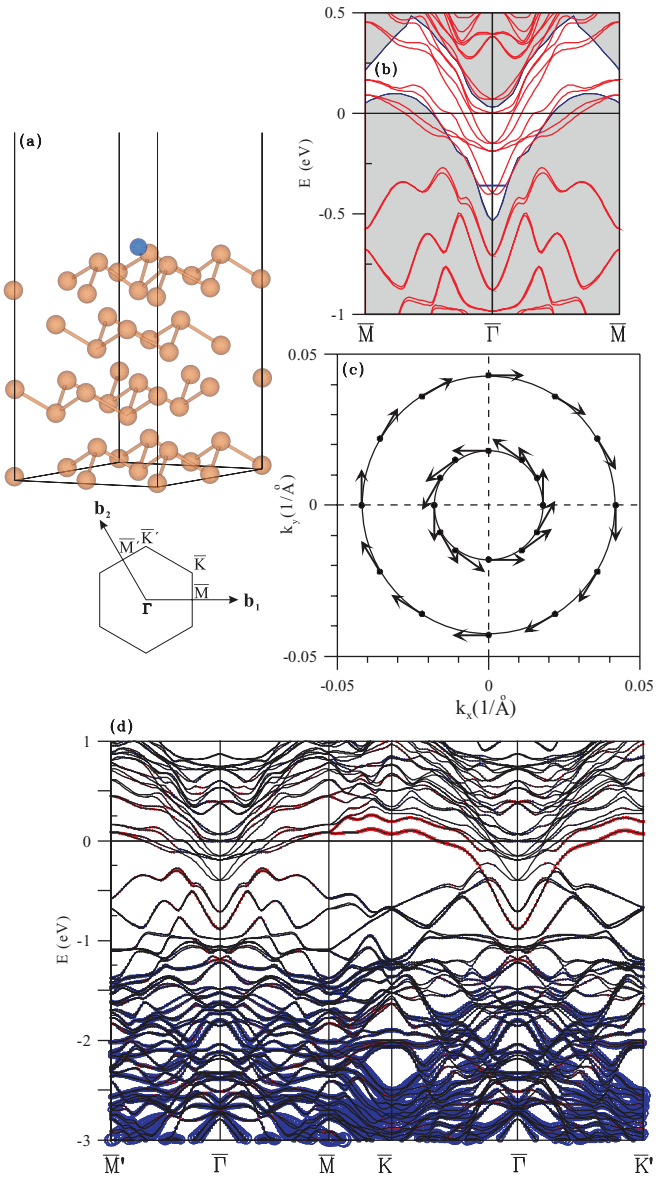

FIG. 4. (Color online) (a) A Cu atom is adsorbed on the top surface of the four -bilayer Sb film in a unit cell of 32 Sb atoms. (b) Energy bands along the $\bar{\Gamma} - \bar{M}$ direction for the adsorption. Two Dirac cones are formed as a result. (c) Spin texture corresponding to the energy indicated by the horizontal bar in (b). (d) Band structure of the configuration shown in (a) along symmetry directions of the Brillouin zone.

energy and of d orbital characters. An exception is found for a band crossing the Fermi level in either the $\bar{\Gamma} - \bar{K}$ or $\bar{\Gamma} - \bar{K}'$ direction comprising a Cu s orbital.

This kind of adsorption-assisted formation of Dirac cones also occurs in the cases of Zn and Ni. Binding energy is a weaker one of only −0.807 eV for Zn, and two Dirac cones are also found [Fig. 5(a)] with the one lower in energy associated mostly with electrons from the Sb atoms of the pristine surface layer. Spin texture analyzed at the energy of −0.225 eV is shown in Fig. 5(b), revealing the same spin-locked chiral structure at each **k** point. Figures 6(a) and 6(b) are energy bands and spin texture for the Ni-adsorbed Sb film. The Dirac cone corresponding to the pristine surface is higher in energy,

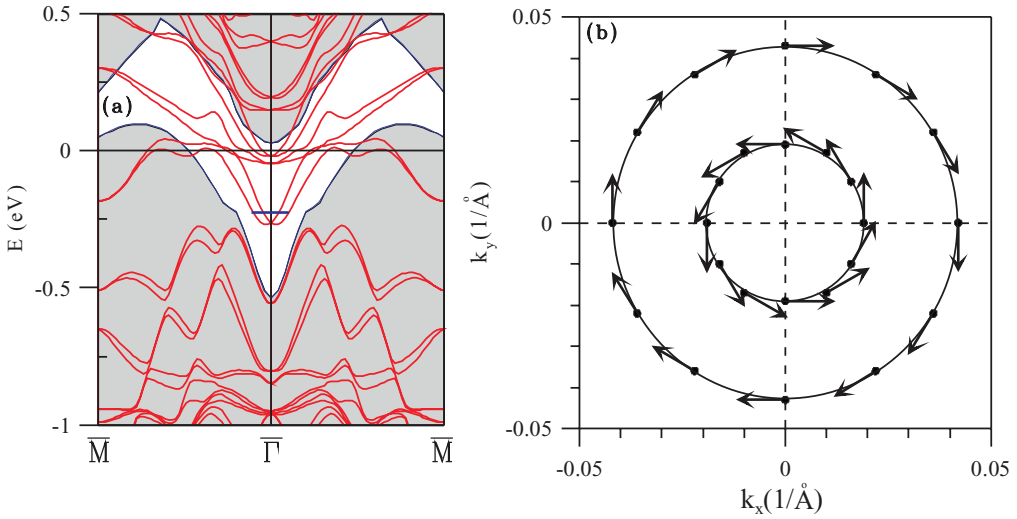

FIG. 5. (Color online) (a) Energy bands along the $\bar{\Gamma} - \bar{M}$ direction for the configuration of Zn adsorption (one Zn atom per unit cell) on the four -bilayer Sb film. (b) Spin texture corresponding to the energy indicated by the horizontal bar in (a).

and the spin texture is also analyzed at a higher energy of only 0.005 eV below the Fermi level. Again, spin angular momenta lie completely in the k_x-k_y plane, and time-reversal symmetry is observed for the two bands associated with the Dirac cone on all **k** points. Figure 7(a) illustrates the distribution of total density of states (DOS) of the Sb film with the Ni adatom. The contribution of the Ni atom can be extracted from Fig. 7(b), which shows that the local DOS (LDOS) of Ni consists overwhelmingly of 3*d* orbitals, and its presence at the Fermi level is negligible. Figure 7(c) is the LDOS taken from a Sb atom on the surface without Ni adsorption. Summed together, the wave functions from surface Sb atoms dominate the bands crossing the Fermi level. It is also a possible scenario that impurity adsorption occurs on both faces of the Sb film.

The four-bilayer Sb film is not a stable structure for such kind of double adsorptions, due to relatively strong quantum tunneling between the two faces. However, in a six-bilayer film deposited on a substrate (simulated by H adsorption as mentioned in Ref. 12) and with a Cu atom attached to the top surface, we find that Dirac cones are also formed and time-reversal symmetry still observed. The spin texture is warped by large out-of-plane components, but the spin is still orthogonal to **k**, and topological conduction is still in effect on both surfaces.

Finally, we considered the adsorption of magnetic atoms. There have been theoretical and experimental studies on the adsorption or doping of magnetic atoms on bulk topological insulators such as Bi_2Se_3[17,18] and Bi_2Te_3,[19] where topological characters remained intact despite the disturbance of the magnetic impurities. For the Sb thin film, the situation was different. In the very robust Sc adsorption, the extremely small magnetic moment did not destroy the time-reversal symmetry of the energy bands, as is shown in Fig. 8(a). But spin texture corresponding to energy at 0.06 eV below the Fermi level

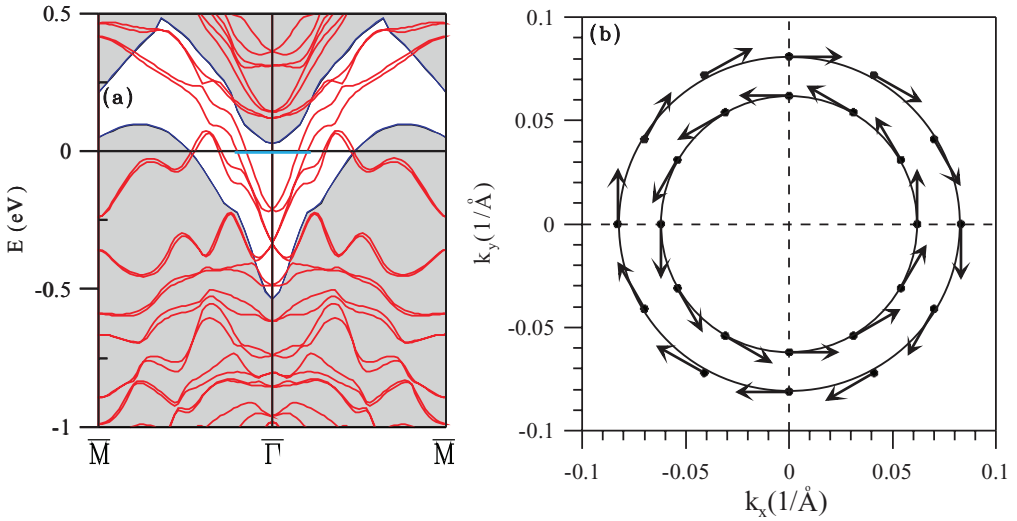

FIG. 6. (Color online) (a) Energy bands along the $\bar{\Gamma} - \bar{M}$ direction for the configuration of Ni adsorption (one Ni atom per unit cell) on the four -bilayer Sb film. (b) Spin texture corresponding to the energy (− 0.005 eV) indicated by the horizontal bar in (a).

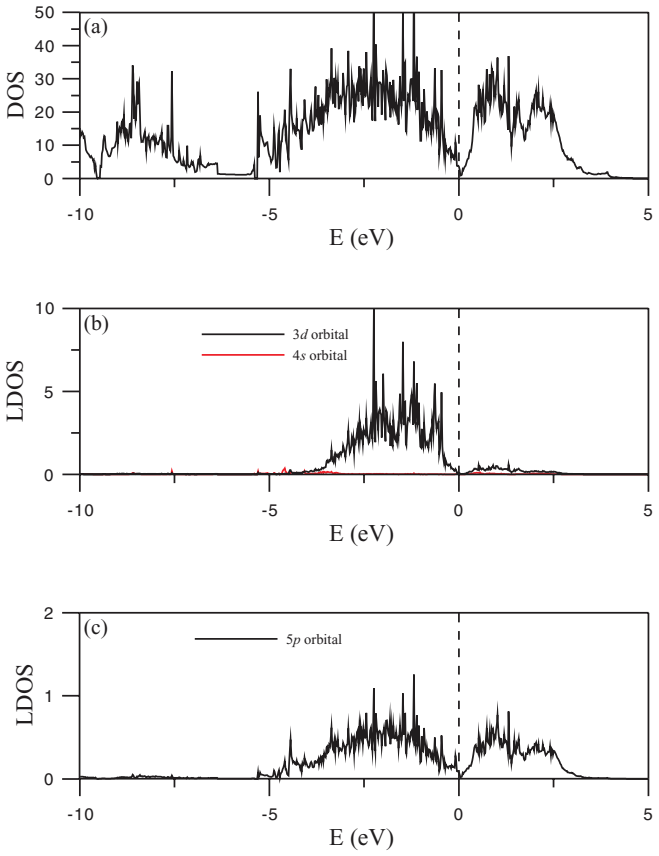

FIG. 7. (Color online) (a) Total DOS of Ni adsorption by the four -bilayer Sb film. LDOS contributed by (b) the Ni adatom and (c) the Sb atom on the pristine surface layer.

[Fig. 8(b)] is greatly distorted from concentric circles. Very large out-of-plane components of spin angular momenta can be found from the figure. For the Co adsorption, with its magnetic moment an order of magnitude larger than that of Sc, but still insignificant compared with the other magnetic TM atoms, no

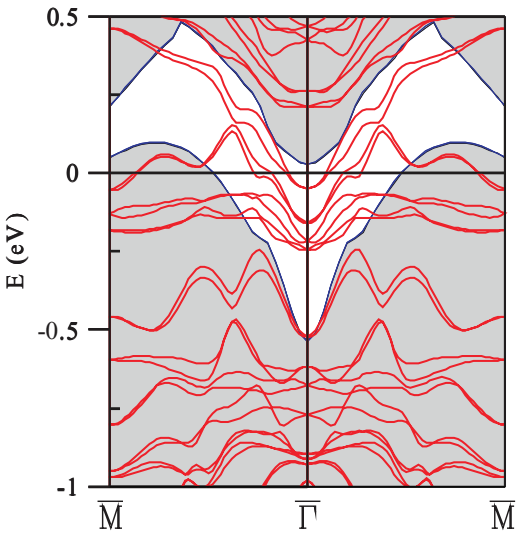

FIG. 9. (Color online) Energy bands along the $\bar{\Gamma} - \bar{M}$ direction for the configuration of Co adsorption (one Co atom per unit cell) on the four-bilayer Sb film.

Dirac cones are formed with bands extending above the Fermi level, as is evident from the band structure in Fig. 9, making topological conduction impossible.

For the other 3*d* TM atoms with large magnetic moments, which are Ti, V, Cr, Mn, and Fe, topological conduction completely disappeared. Two typical examples are selected for discussion. In the adsorption of a Fe atom per expanded unit cell of the four-bilayer Sb film, a magnetic moment of 2.0496 μ_B and binding energy of 4.430 eV are obtained from the calculation. Shown in Fig. 10(a), there are bands converging at the $\bar{\Gamma}$ point, but no Dirac cone is formed. Analysis of the spin texture also clearly indicates breaking of the time-reversal symmetry on equi-energy curves, with large out-of-plane components at some **k** points. An even higher magnetic moment of 3.1366 μ_B is associated with Mn adsorption, which has a binding energy of 3.090 eV,

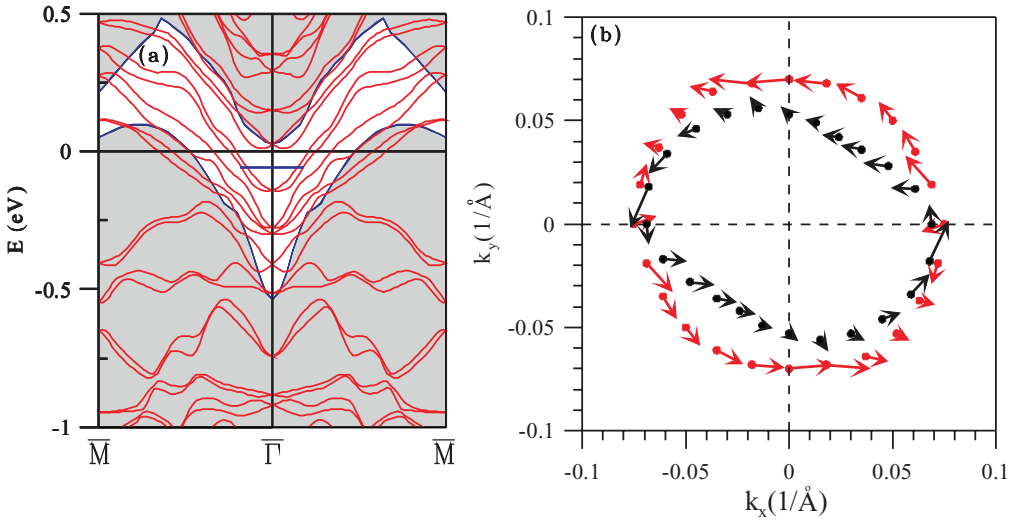

FIG. 8. (Color online) (a) Energy bands along the $\bar{\Gamma} - \bar{M}$ direction for the configuration of Sc adsorption (one Sc atom per unit cell) on the four-bilayer Sb film. (b) Spin texture corresponding to the energy indicated by the horizontal bar in (a).

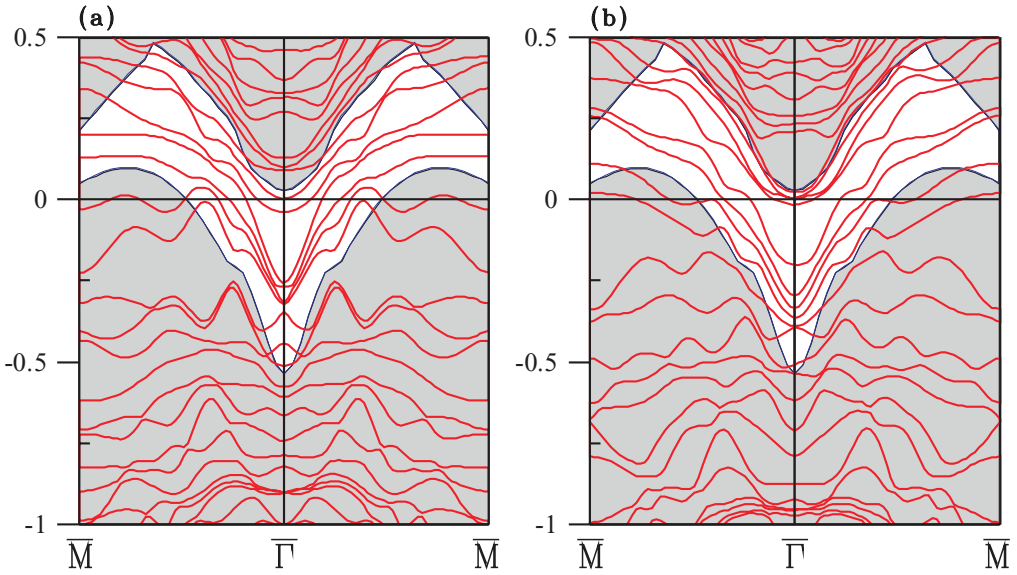

FIG. 10. (Color online) Energy bands along the $\bar{\Gamma} - \bar{M}$ direction for (a) Fe and (b) Mn adsorptions by the four-bilayer Sb film.

causing more splitting of energy bands and skewed crossing bands as revealed in Fig. 10(b). There is also serious violation of time-reversal symmetry for the relevant energy bands, providing further evidence that magnetism and topological surface states do not coexist under such an adsorption of magnetic atoms on the Sb thin film.

In conclusion, our calculations have shown that a four-bilayer Sb thin film can be turned into a conductor with energy bands possessing time-reversal symmetry by the adsorption of H and nonmagnetic 3*d* TM atoms on its surfaces. Adsorption of magnetic TM atoms other than Sc, however, destroys time-reversal symmetry and topological conduction. We have also shown that a nonmagnetic impurity adsorbed on one surface makes possible the formation of Dirac cones and nondissipative transport by suppressing quantum tunneling between the two faces of the thin film. Instead of growing bulky topological insulators with tens or even hundreds of layers of atoms, one has the option of using the very thin films of only a few layers and obtaining topological conduction at the surfaces of the films. This should promote the application of thin films as vehicles of topological conduction in future research.

This work was supported by the National Science Council of the Republic of China under Grant No. NSC 101-2112-M-004-004-MY3. Support from the National Center for Theoretical Sciences and the National Center for High-Performance Computing of the ROC are also gratefully acknowledged.

*Email address: ckyang@nccu.edu.tw

[1]C. L. Kane and E. J. Mele, Phys. Rev. Lett. **95**, 146802 (2005); **95**, 226801 (2005).
[2]B. A. Bernevig and S. C. Zhang, Phys. Rev. Lett. **96**, 106802 (2006).
[3]L. Fu and C. L. Kane, Phys. Rev. B **76**, 045302 (2007).
[4]L. Fu, C. L. Kane, and E. J. Mele, Phys. Rev. Lett. **98**, 106803 (2007).
[5]J. E. Moore and L. Balents, Phys. Rev. B **75**, 121306 (2007).
[6]S. Murakami, New J. Phys. **9**, 356 (2007).
[7]R. Roy, Phys. Rev. B **79**, 195322 (2009).
[8]M. Z. Hasan and C. L. Kane, Rev. Mod. Phys. **82**, 3045 (2010), and references therein.
[9]X. L. Qi and S. C. Zhang, Rev. Mod. Phys. **83**, 1057 (2011), and references therein.
[10]F. Wilczek, Nat. Phys. **5**, 614 (2009).
[11]X. Wang, G. Bian, T. Miller, and T.-C. Chiang, Phys. Rev. Lett. **108**, 096404 (2012).
[12]G. Bian, X. Wang, Y. Liu, T. Miller, and T.-C. Chiang, Phys. Rev. Lett. **108**, 176401 (2012).
[13]G. Kresse and D. Joubert, Phys. Rev. B **59**, 1758 (1999).
[14]G. Kresse and J. Furthmüller, Phys. Rev. B **54**, 11169 (1996).
[15]S. Basak, H. Lin, L. A. Wray, S.-Y. Xu, L. Fu, M. Z. Hasan, and A. Bansil, Phys. Rev. B **84**, 121401(R) (2011).
[16]W. Tang, E. Sanville, and G. Henkelman, J. Phys.: Condens. Matter **21**, 084204 (2009).
[17]M. R. Scholz, J. Sánchez-Barriga, D. Marchenko, A. Varykhalov, A. Volykhov, L. V. Yashina, and O. Rader, Phys. Rev. Lett. **108**, 256810 (2012).
[18]J. Honolka, A. A. Khajetorians, V. Sessi, T. O. Wehling, S. Stepanow, J.-L. Mi, B. B. Iversen, T. Schlenk, J. Wiebe, N. B. Brookes, A. I. Lichtenstein, Ph. Hofmann, K. Kern, and R. Wiesendanger, Phys. Rev. Lett. **108**, 256811 (2012).
[19]J. Henk, M. Flieger, I. V. Maznichenko, I. Mertig, A. Ernst, S. V. Eremeev, and E. V. Chulkov, Phys. Rev. Lett. **109**, 076801 (2012).